



Research article

Interfacial electrochemical properties of natural Moroccan Ghassoul (stevensite) clay in aqueous suspension

Hamou Moussout^{*}, Hammou Ahlafi, Mustapha Aazza, Rachid Chfaira, Chadia Mounir

Laboratory of Chemistry and Biology Applied to the Environment, Faculty of Sciences, Moulay Ismail University, BP 11201-Zitoune, Meknes, 50070, Morocco

ARTICLE INFO

Keywords:

Electrochemistry
 Environmental science
 Ghassoul
 Ions
 Interfacial
 Electrochemical
 Potentiometric
 Titrations conductometric

ABSTRACT

A raw Moroccan clay locally named "Ghassoul" (Gh) was characterized using several techniques such as Fourier Transform Infrared Spectroscopy (FTIR), X-Ray Diffraction (XRD), Brunauer, Emmett and Teller method (BET), Scanning Electron Microscopy (SEM) and simultaneous Thermo-Gravimetric and Differential Thermal Analysis (TGA/DTA). These techniques indicate that the Gh consists essentially of stevensite, calcite, dolomite and quartz. The study of the interfacial electrochemical properties of Gh in different solutions of electrolyte salts (NaCl, CsCl, NaF, NaBr and LiCl) was carried out using the potentiometric and conductometric titrations. It was shown that the Gh particles were stable in aqueous phase within the pH range (3–12) and the point of zero charge (PZC) was located at pH = 10.7. The adsorption sequence, carried out at various ionic strengths, showed that the adsorption mechanism onto the Gh particles is both electrostatic and specific at pH below the pH_{pzc} , while at a pH range greater than the pH_{pzc} the mechanism is electrostatic in nature. The total number of surface sites, determined using the graphical extrapolation method, was $110\text{OH}/\text{nm}^2$. Ionization constants (pK_{int}^+ and pK_{int}^-) in the presence of various electrolytes have also been determined and their values are 10.08 and 12.38, respectively.

1. Introduction

During the past few years, natural aluminosilicate minerals (e.g. clay minerals) have received a great interest in industrial and environmental chemistry because of their abundance, low cost and environmentally friendly nature. It was reported that for each application, the physico-chemical properties of clays, are closely linked to the following factors: (a) their crystal structures, which are classified as 1:1 and 2:1, depending on the built of tetrahedral silicate sheets and octahedral hydroxide sheets, respectively, and (b) their chemical constituents. Among the well-known varieties of clays materials, Gh which can be found only in Jbel Ghassoul in Morocco, is widely used in manufacturing of several products, due to its presence in different dermo cosmetic products, such as facial creams, sunscreen, products for skin cleansing and shampoos etc. According to the first article Moroccan Decree n° 2-73-370 dated March 5th 1974 (Benhammou et al., 2009), the trade name "Ghassoul" is only reserved for the products containing more than 90% of the clay mineral known as stevensite, which has a 2:1-type layer structure (one octahedral sheet between two tetrahedral sheets) and a general chemical composition as: $\text{Mg}_{3-x}\text{Si}_4\text{O}_{10}(\text{OH})_2 \cdot (\text{M}^{y+} \cdot n\text{H}_2\text{O})$, where M is Ca^{2+} , Mg^{2+} , Na^+ , K^+ (López-Galindo et al., 2007; Benhammou et al., 2009).

Due to unique physico-chemical properties of Gh, such as layered structure, swelling behavior, surface charge, high surface area, large cation exchange capacity, high chemical and mechanical stability and its sensitivity to the addition of the electrolytes (Bilgiç, 2005; Viseras et al., 2007), it has found a major advances achieved both in the research domain and applications in many fields, including medicine, catalysis and pharmacy (Leroy and Revil, 2004; Moraes et al., 2017). In most of these applications, Gh is used in aqueous solutions media such for example in the elimination of organic and mineral pollutants from wastewater and the adsorption of toxic heavy metals (López-Durán et al., 2003; Benhammou et al., 2005a, 2005b; Tokarský, 2018), which depend mainly on the physical and chemical properties described above. However, there are no studies have been interested in the study of the electrochemical behavior of Moroccan Gh at the water/Gh interface. As demonstrated by the electrical triple-layer model (TLM), proposed by P. Leroy (Leroy and Revil, 2004), this type of studies reveal the importance of the electrochemical properties of clay minerals to understand a large number of properties of clay-rich porous media and colloidal suspensions of clays. For example, the determination of the electro-kinetic properties of fine particles in an aqueous solution, such as the isoelectric point and the potential-determining ions makes it possible to better understand the

^{*} Corresponding author.

E-mail address: moussouthammou@gmail.com (H. Moussout).

interactions mechanism of inorganic and organic species at the solid-liquid interface, like in the adsorption processes (Azarkan et al., 2016; Kushwaha et al., 2017; Kumar et al., 2019). They also govern other processes such as the flotation, coagulation and dispersion properties in suspension systems. In the ceramic industry and in the design of nanocomposite materials, particularly in clay-water colloidal systems, the electrokinetic properties of colloidal particles identify the optimal conditions of a well-dispersed system. The use of the surface titration of minerals in aqueous electrolyte solutions was considered the best way to investigate the sorption and electrical behavior of minerals. The data are generally collected from acid-base potentiometric and conductometric titrations (Huang and Stumm, 1973; Hiemstra et al., 1989; Avena and De Pauli, 1996, 1998; Du et al., 1997; Lützenkirchen et al., 2002; Duc et al., 2005a, 2005b; 2006; Lützenkirchen, 2005).

Taking into account the numerous applications of Gh, this work aims to study the interfacial electrochemical properties of Gh in aqueous solutions by using acid-base potentiometric and conductometric titrations at 25 °C. In particular, it is intended to determine the parameters such as the insolubility state and the action's nature of the dispersed phase in the dispersing phase, the point of zero charge (pzc) and the total number of surface sites (N_s). The adsorption studies were carried out in the presence of various ions such as Li^+ , Na^+ , Cs^+ , F^- , Cl^- and Br^- . Before these experiments, the raw Gh was characterized using X-rays fluorescence, Fourier Transform Infrared Spectroscopy (FTIR), X-Ray Diffraction (XRD), Scanning Electron Microscopy (SEM) and Brunauer, Emmett and Teller method (BET), and Simultaneous Thermogravimetric and Differential Thermal Analysis (TGA/DTA), was made.

2. Materials and methods

2.1. Chemicals

The Gh used in this work is from the province of Missouri (Morocco) in the locality known as Ksabi. The studied Gh was crowded with a particle size less than 160 μm . The alkali-halide electrolytes NaCl (99.9 %), CsCl (99.9 %), NaF (99.5%), NaBr (99.5 %) and LiCl (99.9 %) used were of analytical grade and supplied by Sigma Aldrich Company. A distilled water with a specific conductivity about 0.5 $\mu\text{S cm}^{-1}$ was used in all the experiments.

2.2. Potentiometric and conductometric titrations

The experimental measurements of electrochemical parameters such as the potentiometric and the conductometric titrations were carried out using a common thermostatic bath that allows us to set the temperature of the suspension to be studied. The latter is contained in specially designed glass ball, which was able to accommodate electrodes for conductivity and pH measurements. The studied suspension was continuously homogenized via a mechanical stirrer. In all cases, the addition of titrant volume was performed with a micropipette ($\Delta V = 0.5\% \text{ mL}$), while the pH and the conductivity of the suspension were measured with a pH-meter (type Microcomputer pH/mV/ORION) and a conductometer (type Inolab cond 730), respectively.

2.3. Determination of surface charge density

The experimental acid-base titration procedure was as follows: 100 \pm 1 mL of a blank solution or aqueous Gh suspension was introduced in a glass ball thermostated at 25 ± 1 °C. A mixture of fixed concentration of blank solution of a given electrolyte and 0.5 ml of HCl (0.5 mol/L) was mixed to 2 g/L of aqueous Gh suspension. The titrant solution (0.2 Mol/L of NaOH) was added as 50 ± 0.005 μL increment until the pH and the conductivity of the solution became constants. The titration experiments were stopped when the pH was around 12.

2.4. Total number of surface sites

The total number of surface sites (N_s) has been determined by using the graphical extrapolation method based on the application of the amphoteric sites model reported by Stumm, Huang and Jenkins (SHJ) (Stumm, 1992). This model takes into account the nature of the electrolytes depending on the action's nature of the solid in dispersing phase. The graphic extrapolation corresponding to Br^- , which was the most adsorbed ion on the positively charged surface, determines the positively charged sites number (N_s^+), while that corresponding to Cs^+ , which was the adsorbed ion on the negatively charged surface, gives the negatively charged sites number (N_s^-). Thus, the total sites number can be expressed as $N_s = N_s^+ + N_s^-$. Following the SHJ's (Stumm, 1992), the obtained linear equations were given as:

$$\text{--For } \text{pH} < \text{pHpzc}: \frac{1}{H^+} = \frac{N_s^+}{\sigma_0} \cdot \frac{1}{K_{\text{int}}^+} - \frac{1}{K_{\text{int}}^+} \quad (1)$$

and

$$\text{--For } \text{pH} > \text{pHpzc}: H^+ = -\frac{N_s^-}{\sigma_0} \cdot K_{\text{int}}^- - K_{\text{int}}^- \quad (2)$$

where K_{int}^+ and K_{int}^- are the intrinsic acidity constants corresponding to the positively and negatively charged surfaces, respectively.

To determine the maximal exchange capacity of adsorbate-adsorbent, N_s is expressed as the number of OH group (nm^2) of the solid, denoted D_s (Eq. 3), as defined by Boisvert et al. (2001):

$$D_s = \frac{\text{Surface sites number}}{\text{surface unit}} = \frac{N_s \cdot N_{\text{Av}}}{A \cdot m_s \cdot 10^{18}} \quad (3)$$

where n_s is the equivalent number of moles of titrated sites, A is the specific surface area of the sample (nm^2/g), m_s (g) is the weight of the solid and N_{Av} the Avogadro's number. So, N_s can be defined as:

$$N_s = \frac{\text{Number of charges} \cdot q}{\text{surface unit}} = \frac{(n \cdot N_{\text{Av}}) \cdot Z \cdot e}{A \cdot m_s} = \frac{F \cdot n_s}{A \cdot m_s} \quad \text{and} \quad n_s = \frac{N_s \cdot A \cdot m_s}{F}$$

Where $F = 96500 \text{ C mol}^{-1}$ and N_s in $\mu\text{C}/\text{cm}^2$, then, the expression of D_s became:

$$D_s = \frac{N_s \cdot A \cdot m_s}{F} \cdot \frac{N_{\text{Av}}}{A \cdot m_s \cdot 10^{18}} = N_s \cdot \frac{N_{\text{Av}}}{F} \cdot 10^{-18} = 6.24 \cdot 10^{-2} \cdot N_s \cdot (\text{OH} / \text{nm}^2)$$

Otherwise the surface charge density (σ_0) is defined as:

$$\sigma_0 = \frac{\text{Number of charge}}{S} = \frac{N_{\text{Av}} \cdot n_i \cdot Z \cdot e}{A \cdot m_s} = \frac{F \cdot C_B \cdot \Delta V}{A \cdot m_s}$$

Where: C_B (mol/L) is the concentration of the titrant solution (NaOH) and $\Delta V (\text{mL}) = V_{\text{blank}} - V_{\text{solid}}$

$$\sigma_0 = \frac{10^6 \cdot 10^{-3} \cdot F \cdot C_B \cdot \Delta V}{10^4 \cdot A \cdot m_s} = 10^{-1} \cdot \frac{F \cdot C_B}{A \cdot m_s} \cdot \Delta V = C_{\text{ste}} \cdot \Delta V$$

And the uncertainty for (σ_0) is given by: $\Delta \sigma_0 = \left(\frac{\sigma_0}{\Delta V}\right) \Delta(\Delta V)$, where $\Delta(\Delta V) = 0.005 \mu\text{L}$, is the uncertainty for the volume of the solution, measured by the micropipette.

2.5. Characterizations of raw Gh

The chemical composition of raw Gh was obtained with an "Axion" type X-ray fluorescence spectrometer, with a dispersion of wavelength (WDS), 20–60 keV tube energy and 10–125 mA current. The morphology of the samples was observed by using scanning electron microscope (SEM Stereoscan S260) combined with energy dispersive X-ray spectroscopy (EDS). X-ray diffraction (XRD) diffractograms were registered using an

X'PERT MPD-PRO wide-angle X-ray powder diffractometer provided with a diffracted beam monochromator and Ni filtered CuK α radiation ($\lambda = 1.5406 \text{ \AA}$). The scanning 2θ angle was ranged between 4° and 70° with a counting time of 2.0 s and steps of 0.02° . Fourier transform infrared (FTIR) spectrophotometer (Shimadzu, JASCO 4100) was used to record the absorption bands spectrum of Gh in the range of $400\text{--}4000 \text{ cm}^{-1}$, with a resolution of 4 cm^{-1} and accumulation of at least 64 scans. The samples were prepared in KBr discs from very well dried mixtures of about 4 % (w/w). A background scan was recorded prior each measurement and subtracted from the sample spectrum. N $_2$ adsorption/desorption isotherm measurements at $T = -196^\circ \text{C}$ were performed using a Micromeritics ASAP 2010. The specific surface area and the average pore diameter were determined according to the standard BET (Brunner Emmett and Teller) and BJH (Barrett, Joyner and Halenda) methods, respectively. The thermal stability of the sample was carried out in air atmosphere in a TA60 SHIMADZU apparatus, which records simultaneously the DTA and TGA curves. The sample was linearly heated from ambient to 900°C ($T = T_0 + \alpha.t$) at the heating rate $\alpha = 20^\circ \text{C}/\text{min}$.

3. Results and discussion

3.1. Characterization of Gh

Table 1 summarizes the chemical composition of Gh determined by XRF analysis. It indicates that Silicon oxide is the major constituent of Gh (53.62%). Sulfur oxide is present with a significant amount (9.87%) followed by a magnesium oxide (8.26%) and aluminum oxide (8.06%). This is a particular composition of Gh clay due to the presence of a magnesium trioctahedral smectite corresponding to stevensite. The loss on ignition (L.O.I) shown in Table 1 corresponds to the loss of mass resulting from the heat treatment of the sample at $T = 1000^\circ \text{C}$. It is observed that the value of L.O.I does not exceed 8%, which reflects that the amount of the organic matter in the Gh sample is low compared to that of mineral fraction. This result agrees with the infrared analyzes which shows the absence of C–H stretching bands ($2800\text{--}2900 \text{ cm}^{-1}$) of organic molecules in Gh sample.

Figure 1 presents the XRD diffractogram of the raw Gh. It was observed that the obtained diffractogram is similar to that recorded by A. Benhammou et al. for the raw Gh (Benhammou et al., 2009). The (060) reflection corresponds to the trioctahedral smectite, showed by a peak at 1.52 \AA (Brown, 1980). The intense peak at $d = 14.9 \text{ \AA}$ and those observed at 4.50 \AA and $d = 2.59 \text{ \AA}$ indicate that raw Gh consists of clay phyllosilicates, characteristic of stevensite. The presence of calcite can be identified at $d = 2.88 \text{ \AA}$, 2.59 \AA , 2.28 \AA and 1.81 \AA . Raw Gh also contains quartz with peaks located at $d = 4.25 \text{ \AA}$ and 3.35 \AA .

Figure 2 shows the FTIR absorbance of the raw Gh recorded within the range of $400\text{--}4000 \text{ cm}^{-1}$. The two bands which appear as shoulders at 3677 and 3625 cm^{-1} correspond to the stretching vibrations of structural hydroxyl of M–OH group ($M = \text{Al, Fe, Mg}$) (Acevedo et al., 2017). The intense band at 3420 cm^{-1} is due to the OH-stretching vibrations of hydration water in the interlayer space, while that at 1640 cm^{-1} is attributed to its deformation vibration (López-Durán et al., 2003; Moraes et al., 2017). In the spectral region between 400 and 1200 cm^{-1} , the intense and sharp peaks observed at 1014 and 456 cm^{-1} are due to Si–O stretching and deformation vibrations in Si–O–Si, respectively. The bands at 456 and 666 cm^{-1} are assigned to Si–O–Mg bending vibration and is related to Mg in the trioctahedral sheet (Brindley and Kikkawa, 1979). The absorption band at 666 cm^{-1} is exhibited only in the case of stevensite in the smectite group (Buey et al., 2000). The absorption band at 1450 cm^{-1} is characteristic of CO stretching of carbonates due to the presence of calcite in Gh. The vibration of Si–O bond in quartz appear at

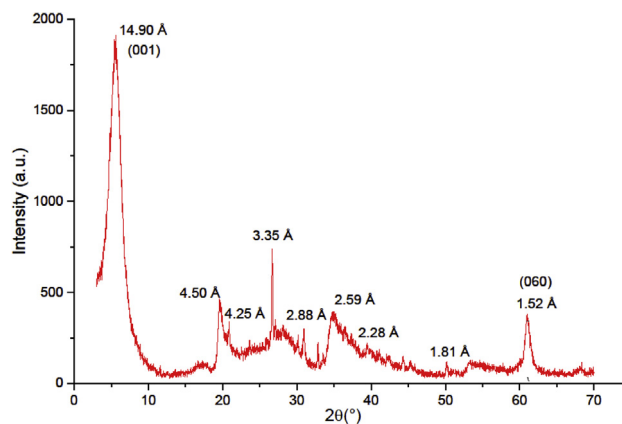


Figure 1. XRD pattern of raw Gh.

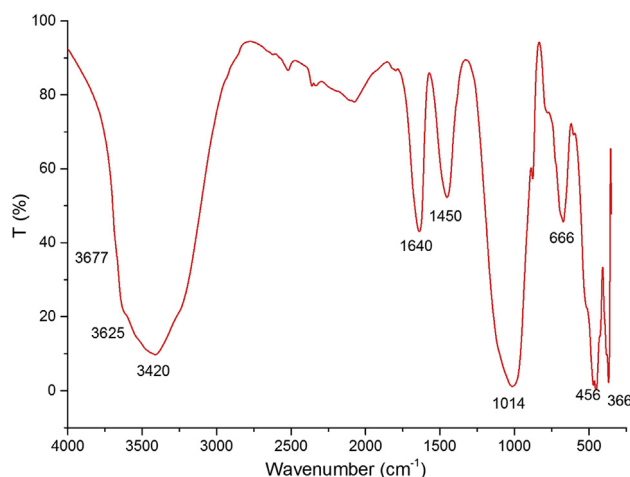


Figure 2. FTIR spectrum of raw Gh.

467 cm^{-1} . It may be noted the total absence of organic matter. The FTIR characterization of the sample was compatible with its composition obtained by XRF analyzes and the value of L.O.I.

Figure 3 shows the N $_2$ adsorption/desorption isotherm recorded for raw Gh sample at $T = 77 \text{ K}$. It was found that the BET surface for raw Gh was $146.70 \text{ m}^2 \text{ g}^{-1}$. The pore diameter distribution, calculated using the BJH method of the desorption isotherm branch (inside Figure 3), was found around 20 and 30 \AA and the total pore volume was $0.11 \text{ cm}^3 \text{ g}^{-1}$. The volume adsorbed in the region of very low relative pressure, $P/P^0 < 0.05$, indicated the presence of some micropores, while at a higher relative pressure, $P/P^0 \geq 0.4$, clear hysteresis loop is observed indicating the presence of mesopores. According to the IUPAC nomenclature (International Union of Pure and Applied Chemistry), this isotherm could be classified as a type IV isotherm. A hysteresis loop of type H2 and a limit of adsorption at high relative pressure (P/P^0) are features of these isotherms, which correspond to the presence of ink-bottle and/or constricted mesopores.

SEM image of raw Gh shown in Figure 4 indicates that Gh particles have an automorphous petaloid-like microstructure, typical of that in smectite clay (Rhouta et al., 2008), and the petals are either present in the form of planar flakes or exhibit folded edges to form a flower-shaped structure. EDX analysis indicates that the Gh consists essentially of silica and magnesium oxide.

Table 1. Chemical composition of raw Gh.

Oxides (%)	SiO $_2$	Fe $_2$ O $_3$	Al $_2$ O $_3$	MgO	ZnO	CaO	Na $_2$ O	K $_2$ O	SO $_3$	L.O.I
Raw Gh	53.62	1.12	8.06	8.26	2.50	5.90	0.72	2.12	9.87	7.83

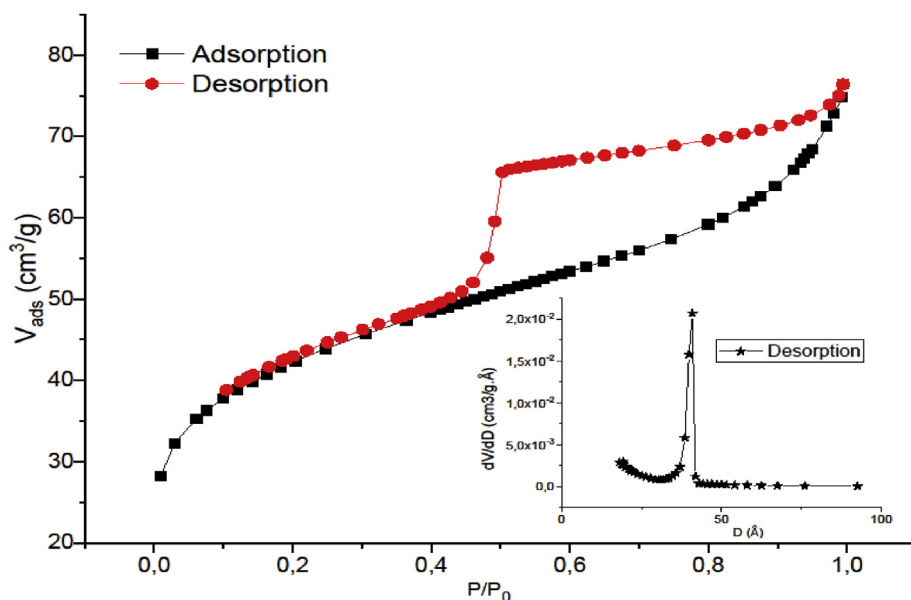


Figure 3. N_2 adsorption/desorption isotherm of raw Gh.

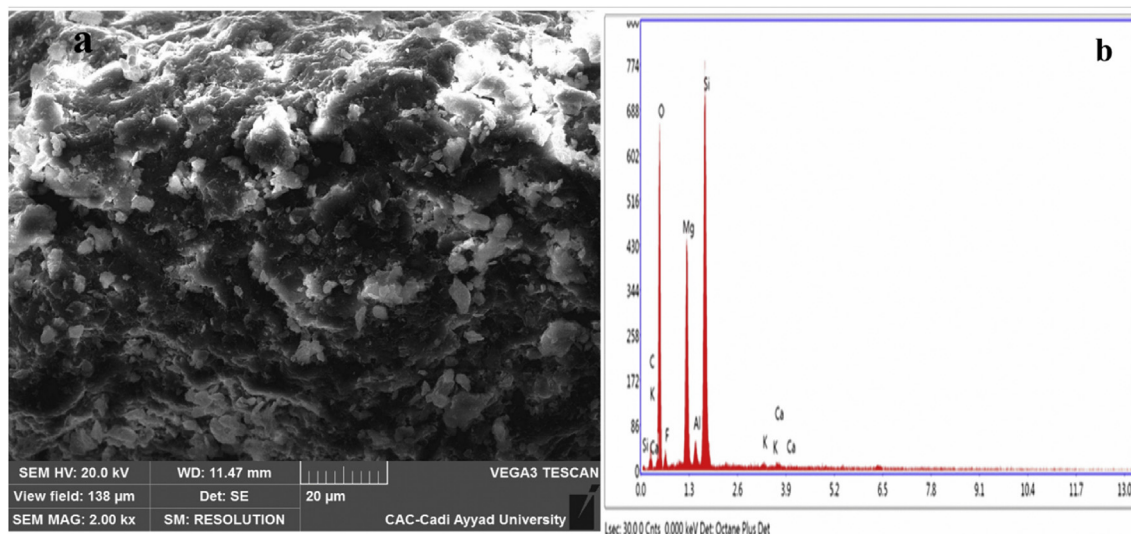


Figure 4. SEM (a) micrograph with EDX (b) analysis of raw Gh.

Thermogravimetric analysis can help to get the information about the thermal stability of the Gh sample. TGA/DTA/DrTGA curves of raw Gh shown in Figure 5 presents 15.68 % of total weight loss when it was heated from $T = 298$ K up to 900 K under a heating rate of 20 K min^{-1} . The first weight loss at 357K in DrTGA corresponds to the desorption of physisorbed water and the second one at 410K corresponds to the loss of the interlayer water. At $T > 440$ K, the 4% mass loss is attributed to the dehydroxylation, and the decomposition of carbonates. In the DTA curve, the first weight loss is associated with two endothermic peaks which are identified at $T = 357$ and 409 K. A large and asymmetric exothermic peak can be seen at $T = 541$ K, it could be due to the dehydroxylation of Gh and the decomposition of carbonates.

3.2. Solubility of Gh particles in dispersing phase

Before each potentiometric or conductimetric titration, the sample was maintained in each dispersing phase for $t = 10$ h, which represents the time needed for the ion exchanges, characterizing the experimental pH parameter, between both dispersed and dispersing phases. Figure 6

represents an example of the evolution of pH vs. the contact time of Gh with NaCl ($C = 10^{-3}$ M), which indicates that the pH remains constant after $t = 100$ min. Avena et al. (Avena and De Pauli, 1998) and El Mragui et al. (El Mragui et al., 2017), obtained an equilibrium time $t > 10$ h with an Argentinean montmorillonite and Moroccan bentonite dispersions, respectively. They explained this behavior, by the edge-to-face interactions between positively charged edges and negatively charged faces.

For a colloidal sol, such as natural Gh in aqueous suspension, the determination of the electrochemical properties at their interface requires the identification of the insolubility domains of the dispersant phase in the dispersing phase. This study was carried out by using conductometric titrations versus the pH of the solution mixtures (Daou et al., 2013). The principle of these measurements was based on the comparison of two types of conductometric titration curves. The first ones are recorded for the blank titrations of aqueous solutions containing various electrolytes (LiCl, NaCl, KCl, CsCl, NaBr and NaF) and 0.5 mL of HCl (0.5 mol/L). The second curves concern the conductometric titrations, recorded in the same experimental conditions, in the presence of 2

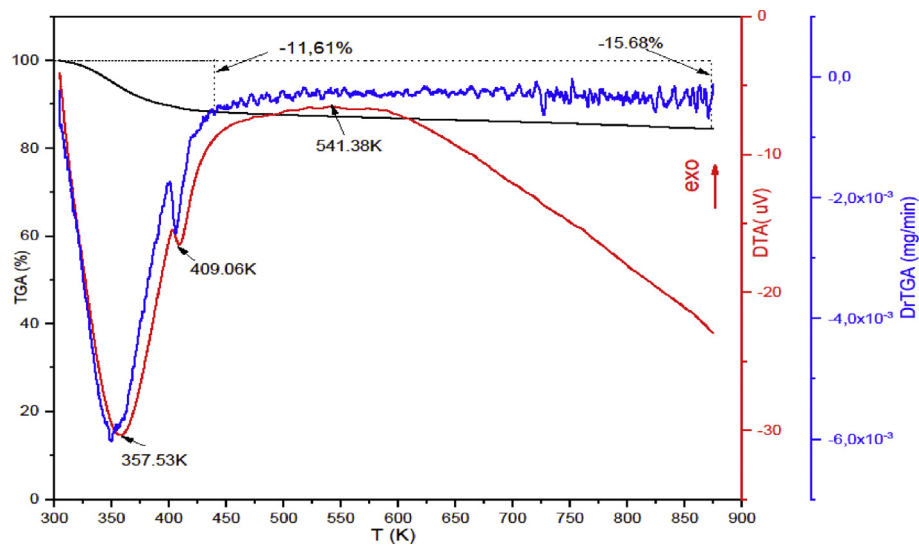


Figure 5. TGA/DTG/DTA of raw Gh.

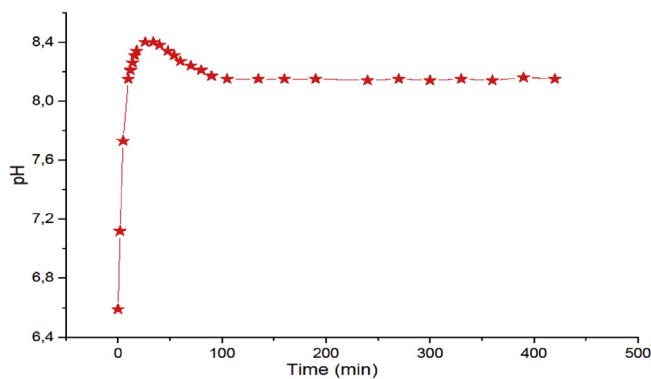


Figure 6. Evolution of pH versus contact time of dispersing (NaCl) in the presence of dispersed phase (Gh).

g/L of Gh. At a given value of pH, the difference in the specific conductivity between the two conductometric titrations curves is due to the conductivity provided both by the determinant ions of the potential (H^+ and OH^-) and the soluble ionic species provided from the solubility of the particles in the dispersing phase. Figure 7 shows the obtained curves of specific conductometric titration for both the blank aqueous solutions and aqueous Gh suspension in the presence of KCl and NaCl at various ionic strengths. The values of parameter (χ) are measured with an accuracy of $\pm 0.5\%$ $\mu S/cm$, given by the conductometer used. From these figures, it can be observed that the difference in the conductivity between blank and Gh solutions depends mainly on the nature and the ionic strength of the electrolyte used. The difference between the specific conductivity recorded for blank solution (χ_{Blank}) and that of aqueous Gh suspensions (χ_{Gh}) is ranged from 10 to 190 $\mu S/cm$, indicating a low concentration of soluble species were released in the solution from Gh in the pH range of 4–10. Thus, it can be concluded that the studied Gh sample can be considered stable in aqueous phase in the considered pH range. This finding is valid since the dissolution of montmorillonitic smectites clay was found limited in the studied pH-range (Rozalen et al., 2009).

3.3. pH at the point of zero charge: pH_{pzc}

It is commonly accepted that when immersed in aqueous solutions, natural clays develop surface charges that originate from the clay phase and from other species naturally contained in its structure (Metz et al.,

2005; Duc et al., 2006; Daou et al., 2015). The surface charge density of substrates is a result of the difference in the potential adsorption of H^+ and OH^- ions. The experimental data of the surface charges were obtained by potentiometric titrations of aqueous suspensions containing a fixed concentration of an electrolyte in the presence and in the absence of Gh particles. The most important parameter used to describe the surface properties of variable charge of minerals is the point of zero charge, which corresponds to the pH (pH_{pzc}) at which the net total particle surface charge density is zero (Essington, 1997; Sposito, 2008). It is known that a surface of clay mineral possesses a net negative charge if the solution pH is greater than its pH_{pzc} and a net positive charge at pH values lower than that of the pH_{pzc} (Morais et al., 1976; Essington, 1997). Since, several methods were used to determine experimentally the $pH(pzc)$ of colloidal suspensions. They are generally based on ion adsorption, potentiometric titration or electrophoretic mobility measurements (Chorover and Sposito, 1995; Appel et al., 2003; Phillips and Sheehan, 2005; Bouby et al., 2010; Kosmulski, 2011). The most experimental approach widely used is that, which is independent of the concentration of the salt. When the volumetric potentiometric titration method is used as a function of the pH and the concentration of the salt, the resulting curves must be intersecting at a single point, which corresponds to the $pH(pzc)$. Figure 8a shows the evolution of the surface charge density (σ_0) for the suspension of Gh particles versus the pH and the ionic strength of the KCl electrolyte. It can be clearly observed, that these surface charge curves pass through a unique point at $pH = 10.7 \pm 0.1$, which correspond to the $pH(pzc)$. El Mragui et al. (El Mragui et al., 2017) observed in their potentiometric titration of bentonite that the pH_{pzc} shifted towards the lowest pH values when the ionic strength of CsCl was increased from 10^{-3} to 10^{-1} mol/L. However, Rhouta et al. (2008) explained that the difference in the value of pH_{pzc} observed for the NE70 membrane compared to the NE20 membrane can be explained by the differences in the ionization degree and the structural of the surface functional groups. In addition, they demonstrated that the use of potentiometric titrations to determine the $pH(pzc)$ is an effective method than electrophoresis measurements made to assess the electrostatic transport of charged ions at the nanofiltration membranes surfaces.

Indeed, the $pH(pzc)$ can be determined using another experimental method, developed recently in our laboratory (Daou et al., 2013). It is based on the conductometric titrations at various ionic forces with and without the presence of the solid. As for metallic oxides, the surface charge results from the unequal adsorption ions determining the potential, such as H^+ and OH^- . Thus, the developed method consists in determining the amount of each ion consumed by different adsorption

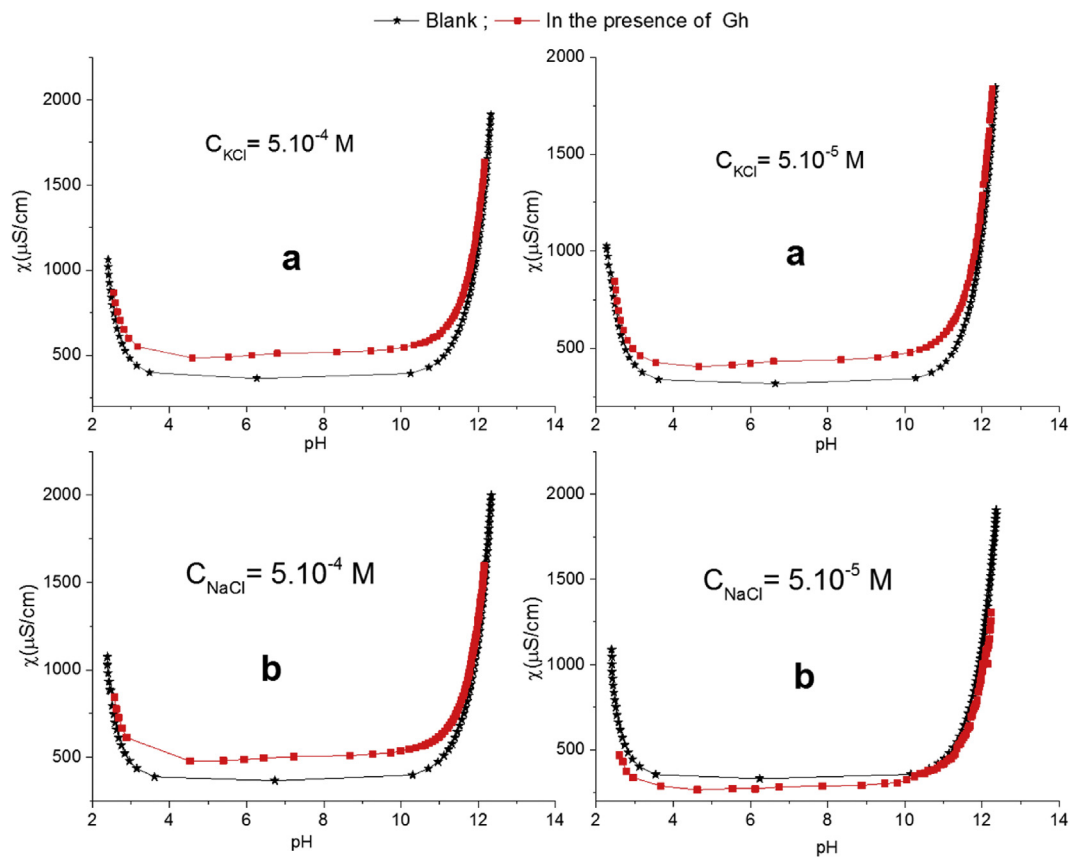


Figure 7. Specific conductometric titration curves obtained for blank aqueous solutions and aqueous suspensions containing 2 g/L of Gh in the presence of KCl (a) and NaCl (b) at two different ionic strengths.

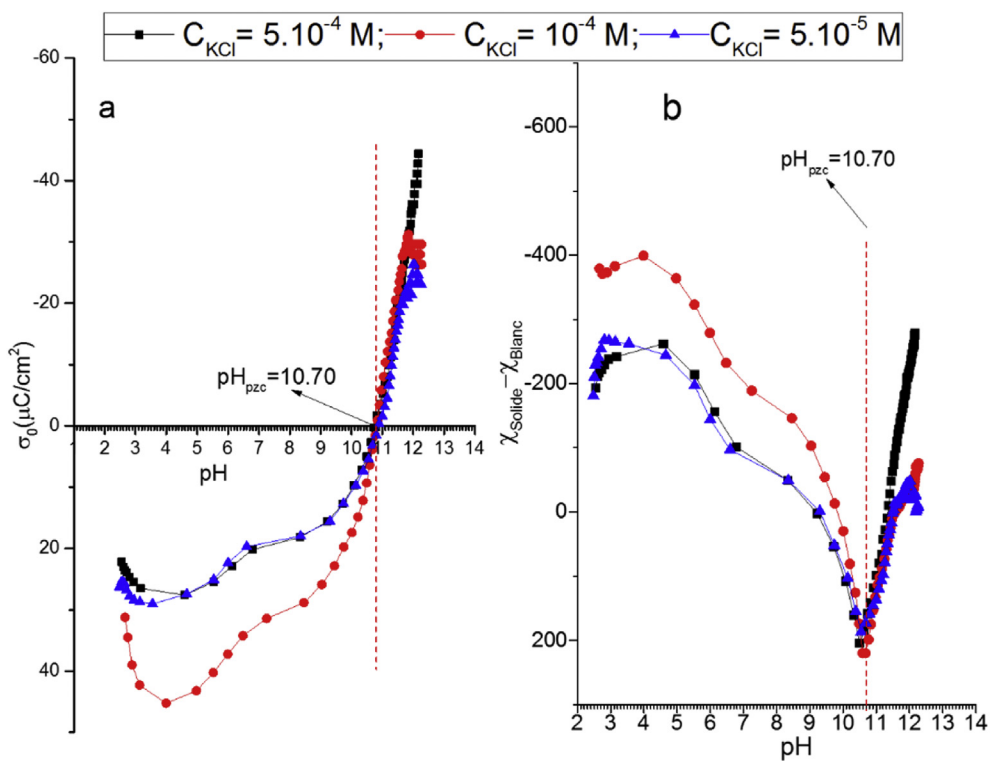


Figure 8. Potentiometric (a) and conductometric (b) titration curves vs pH obtained in the presence of various concentrations of KCl electrolyte and 2 g/L of Gh.

sites of the metallic oxide surface. Figure 8b shows the conductimetric titration curves where it can be observed the difference obtained in the specific conductivity between the blank solution (in absence of solid) and that of the colloidal solution of Gh as function of the pH and the concentration of the KCl salt. It can be noticed that the obtained curves $\Delta\chi$ ($\Delta\chi = \chi_{\text{blank}} - \chi_{\text{solid}}$) vs pH consist of two branches whose minimum is at a common intersection point, in this case at $\text{pH} = 10.7 \pm 0.1$. This value is close to the $\text{pH}(\text{pzc})$ value determined above using the potentiometric titrations method, which confirmed the validity of this method to determine the PZC, as observed in our previous work for bentonite and TiO₂ dispersions, respectively (Daou et al., 2013; El Mragui et al., 2017).

3.4. Effect of the dispersed phase on the dispersing phase

The characterization of the influence of the dispersion of solid phase in the dispersing aqueous solution phase is of great importance to determine the stability of colloidal suspensions. Erkov et al. (2000) indicate in their study that the presence of a permanent hydration layer on the surfaces of the particle suspension increases considerably the stability of the studied hydrosol. In this work, the adsorption studies of cationic (Li^+ , Na^+ , K^+ and Cs^+) and anionic (F^- , Cl^- and Br^-) ions have been carried out for pH values greater and lower than that of pH_{pzc} , respectively. Figure 9a indicates that the anionic adsorption of the three studied anions can be classified as follows: $\text{F}^- < \text{Cl}^- < \text{Br}^-$, suggesting that Br^- was more adsorbed than Cl^- and F^- ions. This result indicates that the anionic adsorption on the studied Gh sample requires the determination of the interactions between: (a) the surface of the Gh and water, (b) the surface of the Gh sample and the ions, and (c) between the ions and water. According to the theoretical models of Evans, Gurney and Gierst's (Dumont et al., 1999; Piasecki et al., 2010), more an ion is adsorbed into an interface, more its action on the structure of the water is similar to that of this interface. Consequently, Br^- , which was the most adsorbed ion on the positively charged surface of Gh could be classified as a structure breaker of the water (Lyklema, 2009). Therefore, the natural Gh particles studied in aqueous phase behave at a pH lower than the pH_{pzc} as disorganizing particles of the water structure according to an adsorption mechanism involving specific

electrostatic interactions. However, at pH greater than that of pH_{pzc} the adsorption sequence of various cationic strengths (Li^+ , Na^+ , K^+ and Cs^+ cations) lead to the curves represented in Figure 9b. The sequence of the adsorption of these cations onto the surface of Gh showed that the adsorption mechanism is only electrostatic and not specific, because the surface charge density developed by these cations is relatively similar.

3.5. Total number of surface sites

The total number of surface sites (N_s) has been determined by using the linear Eqs. (1) and (2). Figures 10a,b show that the plot of experimental points, respectively for Br^- and Cs^+ . It can be noticed that these data follow straight lines, with a coefficient of determination ($R^2 > 0.97$), in good accordance with the preceding equations. The calculated values of N_s^- and N_s^+ for the adsorption of Br^- and Cs^+ from their corresponding equations are, respectively 144 and $32 \mu\text{C}/\text{cm}^2$, thus the total density of surface sites of the Gh is:

$$N_s = N_s^- + N_s^+ = 176 \mu\text{C}/\text{cm}^2$$

The maximal exchange capacity of adsorbate-adsorbent can be determined by using Eq. (3):

$$D_s = N_s \cdot \frac{N_{Av}}{F} \cdot \frac{10^{-18} \text{OH}}{\text{nm}^2} = 11 \left(\frac{\text{OH}}{\text{nm}^2} \right)$$

The ionization constants have been also determined by applying this graphical extrapolation method. The values of $\text{p}K_{\text{int}}^+$ and $\text{p}K_{\text{int}}^-$ obtained for the aqueous suspension of Gh in the presence of various electrolytes are 10.08 and 12.38, respectively ($\Delta\text{p}K = \text{p}K_{\text{int}}^- - \text{p}K_{\text{int}}^+ = 2.3$). The comparison of the calculated values of $\Delta\text{p}K$ with those found by Waychunas et al. and Malgat et al. in the case of organizing oxides (Waychunas et al., 2002; Malgat et al., 2004), indicate that the $\Delta\text{p}K$ is an intrinsic surface property to each colloidal suspension. It is also noticed that the value of $\Delta\text{p}K$ is less than 4, which is in good agreement with the high measured value of $N_s = 11 \text{ OH}/\text{nm}^2$. This result is in accordance with several works (Kallay and Žalac, 2000) suggesting that the oxides which have a relatively low density of sites

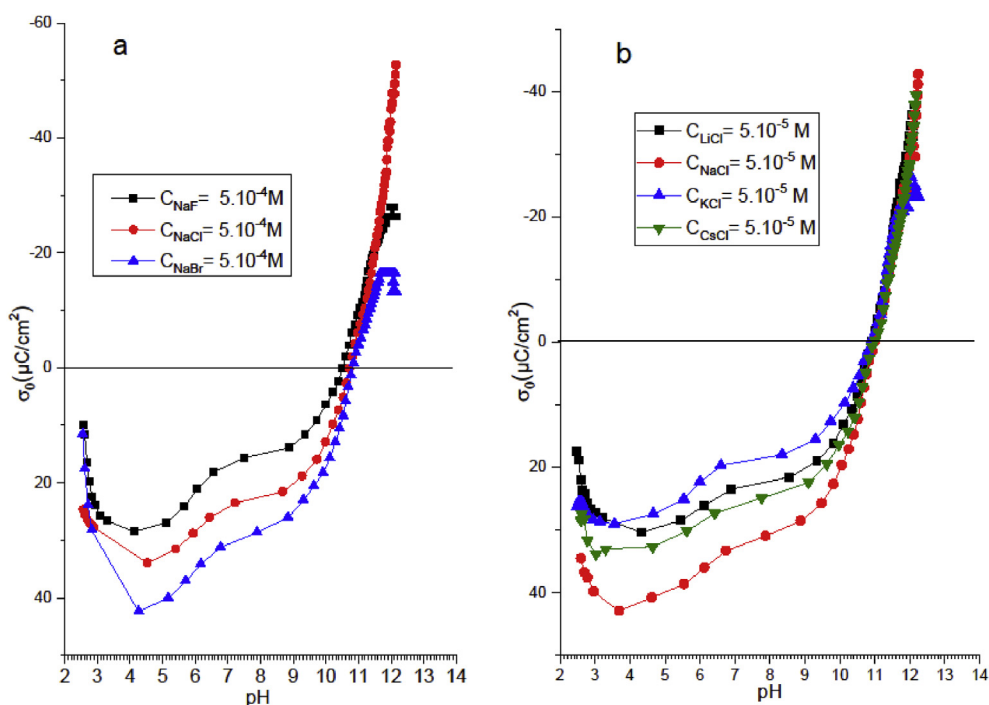


Figure 9. Anionic (a) and cationic (b) adsorption sequence in the presence of Gh sample at pH range below and above of pH_{pzc} , respectively.

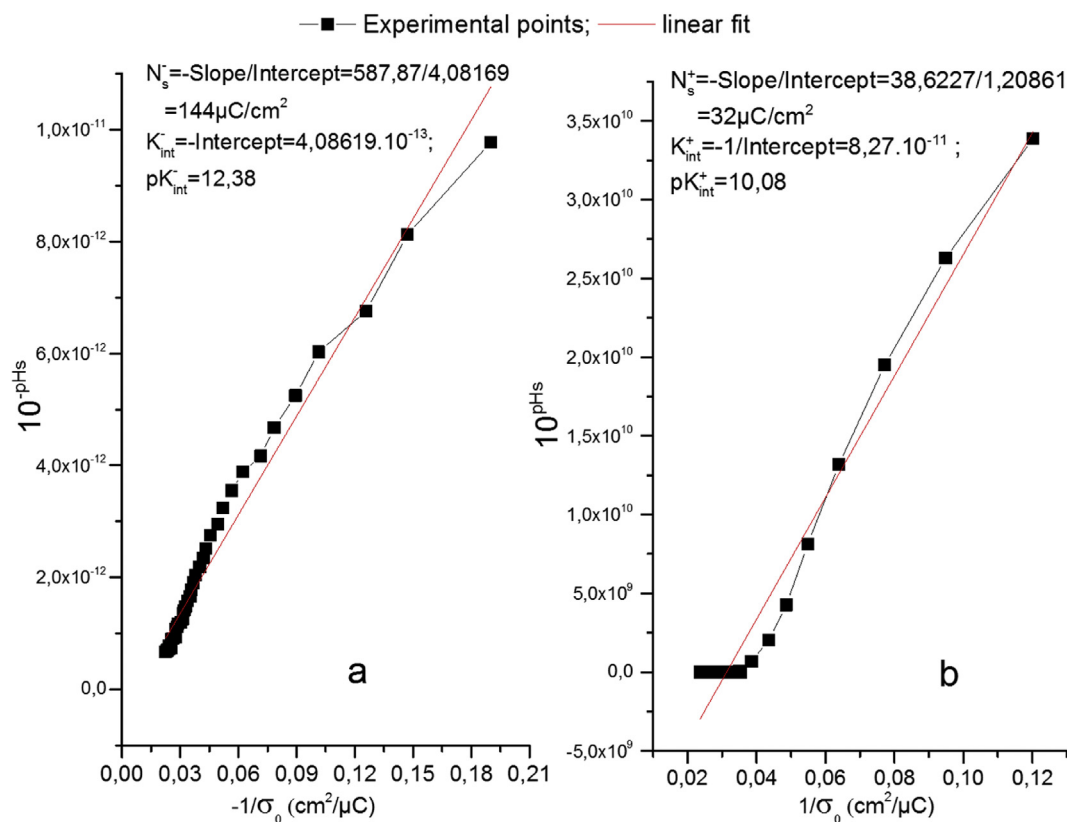


Figure 10. Total density of surface sites $N_s = N_s^- + N_s^+$: N_s^- /Gh in the presence of CsCl (a) and N_s^+ /Gh in the presence of NaBr (b).

(N_s), as in the case of the studied TiO_2 nanoparticles, are characterized by a value of $\Delta pK > 4$ (Daou et al., 2013).

4. Conclusion

In this work, the surface charge properties of raw Moroccan Ghassoul (Gh) were characterized using potentiometric and conductometric titrations methods at a wide range of pH values and under varying ionic strength conditions. The conductometric studies showed that the studied samples can be considered stable in aqueous phase in the studied pH range (3–12). The value of the intrinsic pH_{pzc} measured at 25 °C by using acid-base potentiometric and conductometric titrations was found the same and it was in the order of $10,7 \pm 0,1$. This result demonstrate that the conductometric titrations can be used as an effective method to quantify the interfacial surface charge of clay dispersions in the same way as the potentiometric method.

The value of N_s , deduced from graphical extrapolation method, was found to be equal to $11 \text{ OH}/nm^2$, which reflects a significant exchange capacity (adsorbate-adsorbent) and an action of the structuring dispersed phase on the dispersing phase. The ionic adsorption sequence at different ionic forces, showed a disorganizing action nature of the Gh particles on the dispersing phase and their adsorption mechanism on the solid was exclusively electrostatic in nature at pH greater than the pH_{pzc} value. In contrast, the adsorption mechanism of ions was both electrostatic and specific in nature at pH below the pH_{pzc} value. The value of $\Delta pK = pK_{int}^+ - pK_{int}^-$ was found lower than 4, due to the highest value of the total number of sites (N_s).

Declarations

Author contribution statement

Mustapha Aazza, Chadia Mounir: Conceived and designed the experiments; Performed the experiments.

Hammou Ahlafi, Rachid Chfaira: Analyzed and interpreted the data; Contributed reagents, materials, analysis tools or data; Wrote the paper.

Hamou Moussout: Conceived and designed the experiments; Performed the experiments; Analyzed and interpreted the data; Contributed reagents, materials, analysis tools or data; Wrote the paper.

Funding statement

This research did not receive any specific grant from funding agencies in the public, commercial, or not-for-profit sectors.

Competing interest statement

The authors declare no conflict of interest.

Additional information

No additional information is available for this paper.

References

- Acevedo, N.I.A., Rocha, M.C.G., Bertolino, L.C., 2017. Mineralogical characterization of natural clays from Brazilian Southeast region for industrial applications. *Cerâmica* 63, 253–262.
- Appel, C., Ma, L.Q., Rhue, R.D., Kennelley, E., 2003. Point of zero charge determination in soils and minerals via traditional methods and detection of electroacoustic mobility. *Geoderma* 113, 77–93.
- Avena, M.J., De Pauli, C.P., 1998. Proton adsorption and electrokinetics of an Argentinean montmorillonite. *J. Colloid Interface Sci.* 202, 195–204.
- Avena, M.J., De Pauli, C.P., 1996. Modeling the interfacial properties of an amorphous aluminosilicate dispersed in aqueous NaCl solutions. *Colloids Surfaces A Physicochem. Eng. Asp.* 118, 75–87.
- Azarkan, S., Peña, A., Draoui, K., Sainz-Díaz, C.I., 2016. Adsorption of two fungicides on natural clays of Morocco. *Appl. Clay Sci.* 123, 37–46.
- Benhammou, A., Tanouti, B., Nibou, L., Yaacoubi, A., Bonnet, J.P., 2009. Mineralogical and physicochemical investigation of mg-smectite from jbel ghassoul, Morocco. *Clay Miner.* 57, 264–270.

- Benhammou, A., Yaacoubi, A., Nibou, L., Tanouti, B., 2005a. Study of the removal of mercury(II) and chromium(VI) from aqueous solutions by Moroccan stevensite. *J. Hazard Mater.* 117, 243–249.
- Benhammou, A., Yaacoubi, A., Nibou, L., Tanouti, B., 2005b. Adsorption of metal ions onto Moroccan stevensite: kinetic and isotherm studies. *J. Colloid Interface Sci.* 282, 320–326.
- Bilgiç, C., 2005. Investigation of the factors affecting organic cation adsorption on some silicate minerals. *J. Colloid Interface Sci.* 281, 33–38.
- Boisvert, J.P., Malgat, A., Pochard, L., Daneault, C., 2001. Influence of the counter-ion on the effective charge of polyacrylic acid in dilute condition. *Polymer (Guildf)* 43, 141–148.
- Bouby, M., Lützenkirchen, J., Dardenne, K., Preocanin, T., Denecke, M.A., Klenze, R., Geckeis, H., 2010. Sorption of Eu(III) onto titanium dioxide: measurements and modeling. *J. Colloid Interface Sci.* 350, 551–561.
- Brindley, G.W., Kikkawa, S., 1979. A crystal-chemical study of Mg,Al and Ni,N hydroxy-perchlorates and hydroxy-carbonates. *Am. Mineralogist* 64, 836–843.
- Brown, G., 1980. X-ray diffraction procedures for clay mineral identification. In: *Crystal Structures of Clay Minerals and Their X-Ray Identification*, pp. 305–359.
- Buey, C.D.E.S., Barrios, M.S., Romero, E.G., Montoya, M.D., 2000. Mg-rich smectite “precursor” phase in the Tagus basin, Spain. *Clay Clay Miner.* 48, 366–373.
- Chorover, J., Sposito, G., 1995. Surface-charge characteristics of kaolinitic tropical soils. *Geochem. Cosmochim. Acta* 59, 875–884.
- Daou, I., Chfaira, R., Zegaoui, O., Aouni, Z., Ahlafi, H., 2013. Physico-chemical characterization and interfacial electrochemical properties of nanoparticles of anatase-TiO₂ prepared by the sol-gel method. *Mediterr. J. Chem.* 2, 569–582.
- Daou, I., Zegaoui, O., Chfaira, R., Ahlafi, H., Moussout, H., 2015. Physico-chemical characterization and kinetic study of methylene blue adsorption onto a Moroccan Bentonite. *Int. J. Sci. Res. Publ.* 5, 1–9.
- Du, Q., Sun, Z., Forsling, W., Tang, H., 1997. Adsorption of copper at aqueous illite surfaces. *J. Colloid Interface Sci.* 187, 232–242.
- Duc, M., Gaboriaud, F., Thomas, F., 2005a. Sensitivity of the acid-base properties of clays to the methods of preparation and measurement: 2. Evidence from continuous potentiometric titrations. *J. Colloid Interface Sci.* 289, 148–156.
- Duc, M., Gaboriaud, F., Thomas, F., 2005b. Sensitivity of the acid-base properties of clays to the methods of preparation and measurement: 1. Literature review. *J. Colloid Interface Sci.* 289, 139–147.
- Duc, M., Thomas, F., Gaboriaud, F., 2006. Coupled chemical processes at clay/electrolyte interface: a batch titration study of Na-montmorillonites. *J. Colloid Interface Sci.* 300, 616–625.
- Dumont, F., Verbeiren, P., Buess-Herman, C., 1999. Adsorption sequence of the alkali cations at the tungsten trioxide-water interface. *Colloids Surfaces A Physicochem. Eng. Asp.* 154, 149–156.
- El Mragui, A., Daou, I., Chfaira, R., Zegaoui, O., 2017. Interfacial electrochemical properties of a Moroccan bentonite in aqueous suspension. *J. Mater. Environ. Sci.* 8, 3138–3150.
- Erkov, V.G., Devyatova, S.F., Molodstova, E.L., Malsteva, T.V., Yanovskii, U.A., 2000. Si-TiO₂ interface evolution at prolonged annealing in low vacuum or N₂O ambient. *Appl. Surf. Sci.* 166, 51–56.
- Essington, M.E., 1997. *Environmental Soil Chemistry*. Soil Sci.
- Hiemstra, T., De Wit, J.C.M., Van Riemsdijk, W.H., 1989. Multisite proton adsorption modeling at the solid/solution interface of (hydr)oxides: a new approach. II. Application to various important (hydr)oxides. *J. Colloid Interface Sci.* 133, 105–117.
- Huang, C.P., Stumm, W., 1973. Specific adsorption of cations on hydrous γ -Al₂O₃. *J. Colloid Interface Sci.* 43, 409–420.
- Kallay, N., Zálac, S., 2000. Charged surfaces and interfacial ions. *J. Colloid Interface Sci.*
- Kosmulski, M., 2011. The pH-dependent surface charging and points of zero charge. V. Update. *J. Colloid Interface Sci.* 353, 1–15.
- Kumar, M., Goswami, L., Singh, A.K., Sikandar, M., 2019. Valorization of coal fired-fly ash for potential heavy metal removal from the single and multi-contaminated system. *Heliyon* 5, e02562.
- Kushwaha, A., Rani, R., Kumar, S., Thomas, T., David, A.A., Ahmed, M., 2017. A new insight to adsorption and accumulation of high lead concentration by exopolymer and whole cells of lead-resistant bacterium *Acinetobacter junii* L. Pb1 isolated from coal mine dump. *Environ. Sci. Pollut. Res.* 24, 10652–10661.
- Leroy, P., Revil, A., 2004. A triple-layer model of the surface electrochemical properties of clay minerals. *J. Colloid Interface Sci.* 270, 371–380.
- de López-Durán, J.D.G., Khaldoun, A., Kerkeb, M.L., Ramos-Tejada, M. del M., González-Caballero, F., 2003. Wettability of montmorillonite clays in humic acid solutions. *Clay Clay Miner.* 51, 65–74.
- López-Galindo, A., Viseras, C., Cerezo, P., 2007. Compositional, technical and safety specifications of clays to be used as pharmaceutical and cosmetic products. *Appl. Clay Sci.* 36, 51–63.
- Lützenkirchen, J., 2005. On derivatives of surface charge curves of minerals. *J. Colloid Interface Sci.* 290, 489–497.
- Lützenkirchen, J., Boily, J.F., Lövgren, L., Sjöberg, S., 2002. Limitations of the potentiometric titration technique in determining the proton active site density of goethite surfaces. *Geochem. Cosmochim. Acta* 66, 3389–3396.
- Lyklema, J., 2009. Simple hofmeister series. *Chem. Phys. Lett.* 467, 217–222.
- Malgat, A., Boisvert, J.P., Daneault, C., 2004. Specific influence of univalent cations on the ionization of alumina-coated TiO₂ particles and on the adsorption of poly(acrylic acid). *J. Colloid Interface Sci.* 269, 320–328.
- Metz, V., Amram, K., Ganor, J., 2005. Stoichiometry of smectite dissolution reaction. *Geochem. Cosmochim. Acta* 69, 1755–1772.
- Moraes, J.D.D., Bertolino, S.R.A., Cuffini, S.L., Ducart, D.F., Bretzke, P.E., Leonardi, G.R., 2017. Clay minerals: properties and applications to dermocosmetic products and perspectives of natural raw materials for therapeutic purposes—a review. *Int. J. Pharm.* 534, 213–219.
- Moras, F.I., Page, A.L., Lund, L.J., 1976. The effect of pH, salt concentration, and nature of electrolytes on the charge characteristics of Brazilian tropical soils. *Soil Sci. Soc. Am. J.* 40, 521–527.
- Phillips, I.R., Sheehan, K.J., 2005. Importance of surface charge characteristics when selecting soils for wastewater re-use. *Aust. J. Soil Res.* 43, 915–927.
- Piasecki, W., Zarzycki, P., Charnas, R., 2010. Adsorption of alkali metal cations and halide anions on metal oxides: prediction of Hofmeister series using 1-pK triple layer model. *Adsorption* 16, 295–303.
- Rhouta, B., Kaddami, H., Elbarqy, J., Amjoud, M., Daoudi, L., Maury, F., Senocq, F., Maazouz, A., Gerard, J.-F., 2008. Elucidating the crystal-chemistry of Jbel Rhassoul stevensite (Morocco) by advanced analytical techniques. *Clay Miner.* 43, 393–403.
- Rozalen, M., Huertas, F.J., Brady, P.V., 2009. Experimental study of the effect of pH and temperature on the kinetics of montmorillonite dissolution. *Geochem. Cosmochim. Acta* 73, 3752–3766.
- Sposito, G., 2008. *The Chemistry of Soils*, Sposito, G. 2008. *The Chemistry of Soils*, 2nd Ed. Oxford University Press, New York, p. 330.
- Stumm, W., 1992. *Chemistry of the Interface Processes at the Mineral-Water*, New York.
- Tokarský, J., 2018. Ghassoul – Moroccan clay with excellent adsorption properties. *Mater. Today Proc.* 5, S78–S87.
- Viseras, C., Aguzzi, C., Cerezo, P., Lopez-Galindo, A., 2007. Uses of clay minerals in semisolid health care and therapeutic products. *Appl. Clay Sci.* 36, 37–50.
- Waychunas, G.A., Fuller, C.C., Davis, J.A., 2002. Surface complexation and precipitate geometry for aqueous Zn(II) sorption on ferrihydrite I: X-ray absorption extended fine structure spectroscopy analysis. *Geochem. Cosmochim. Acta* 66, 1119–1137.